SACLANTCEN MEMORANDUM
serial no.: SM-287

SACLANT UNDERSEA
RESEARCH CENTRE

MEMORANDUM

Reverberation suppression

I.P. Kirsteins

April 1995

The SACLANT Undersea Research Centre provides the Supreme Allied Commander Atlantic (SACLANT) with scientific and technical assistance under the terms of its NATO charter, which entered into force on 1 February 1963. Without prejudice to this main task – and under the policy direction of SACLANT – the Centre also renders scientific and technical assistance to the individual NATO nations.

Page count for SM-287 (excluding Covers and Data Sheet)

Pages	Total
i–vii	7
1–11	11
	18

SACLANT Undersea Research Centre
Viale San Bartolomeo 400
19138 San Bartolomeo (SP), Italy

tel: +39-187-540.111
fax: +39-187-524.600

e-mail: sti@saclantc.nato.int

NORTH ATLANTIC TREATY ORGANIZATION

SACLANTCEN SM-287

Reverberation suppression

I.P. Kirsteins

The content of this document pertains to work performed under Project 02 of the SACLANTCEN Programme of Work. The document has been approved for release by The Director, SACLANTCEN.

Issued by:
Systems Research Division

R. Weatherburn
Division Chief

intentionally blank page

Reverberation suppression

I.P. Kirsteins

Executive Summary: We propose a signal processing methodology in which reverberation suppression algorithms are developed using acoustic propagation and scattering physics as a *guide* to model and determine simpler representations for the received data (i.e., reverberation and target waveforms), for which the criteria is applicability or development of efficient adaptive algorithms. The philosophy used here is that it is important to utilize as much prior propagation and scattering information as is practical to improve performance and also use the predicted waveform structures to justify the algorithms being used. This methodology is demonstrated by showing that temporally spread reverberation components, spread either due to the medium and/or extended scatterers, can be accurately modeled using a reduced-rank representation and expansion by discrete prolate spheroidal sequences. These representations lead to simple and efficient algorithms for reverberation suppression and target localization. Theoretical analysis and computer simulation results indicate that these algorithms perform well.

An important advantage of this approach is that prior environmental information can be utilized in a computationally efficient manner, while at the same time adaptively compensating for uncertainty in the environmental information. This is in contrast to a standard matched-field processing approach where the uncertainty in environmental information would have to be compensated by possibly a very high order multidimensional search. Thus the proposed approach is particularly useful in shallow water where acoustic propagation has considerable interaction with the ocean bottom, but the prior bathymetry information can be limited, e.g., bathymetry and sediment properties are coarsely sampled.

One potential scenario envisioned for application of these techniques is where a hostile submarine is stalking a strait or harbor entrance and exploits reverberation from bottom features (e.g., shoals, trenches, cliffs, etc.) to avoid detection.

intentionally blank page

Reverberation suppression

I.P. Kirsteins

Abstract: We propose a processing methodology for shallow-water reverberation suppression in which acoustic propagation and scattering physics are used as a *guide* to develop simple, but still accurate representations for the received data which are motivated by the ease of development of efficient signal-processing algorithms. The methodology is demonstrated by showing that temporally spread reverberation components can be accurately modeled using a reduced-rank representation and expansion by discrete prolate spheroidal sequences. These representations lead to the application of the Principal Component Inverse (PCI) method and the reduced-rank generalized likelihood-ratio test (RR-GLRT) for suppressing reveberation and the development of an iterative scheme for estimating arrival times in the presence of temporally spread reverberation components. We also present a performance analysis of the RR-GLRT. Using both simulated and real data, it is shown that these methods perform well.

Keywords: adaptive detection ○ generalized likelihood-ratio test ○ performance assessment ○ reduced-rank interference cancellation ○ reverberation suppression ○ time delay estimation

Contents

Preface

This memorandum is a collection of three recently presented conference papers on new methods for interference suppression and target localization. The objective of this memorandum is to make available and tie together the work presented in these papers under the common theme of improving target detection and localization in shallow-water reverberation and show how the algorithms are applied to reverberation suppression and target localization. Particular emphasis is given to the special problems of shallow-water reverberation and the methodologies for dealing with shallow-water reverberation.

The remainder of this memorandum consists of an introduction, conclusion and appendix followed by the three papers: (1) *Model-Aided Data Adaptive Suppression of Reverberation* presented at the Low Frequency Active Sonar Conference, SACLANT Undersea Research Centre, La Spezia, Italy, May 1993, (2) *Modeling and Suppression of Reveberation Components* presented at the Seventh SP Workshop on Statistical Signal and Array Processing, Quebec City, QC, Canada, June 1994, and (3) *Analysis and Interpretation of the Reduced-Rank Generalized Likelihood-Ratio Test* presented at the VII European Signal Processing Conference, University of Edinburgh, Scotland, UK, September 1994.

1 Introduction

Standard active sonar systems typically perform poorly in shallow-water environments. The principal cause of poor performance in shallow water are the high levels of bottom reverberation. Bottom reverberation is particularly severe in shallow water because of the numerous interactions of the transmitted acoustic pressure field with the seafloor. Of particular importance are 'target-like' reverberation components due to distinct bathymetric features (e.g., seamounts, cliffs, trenches, pinnacles, etc.). These 'target-like' components lead to masking of true submarine echos and high false alarm rates. This is illustrated in Fig. 1 by the beamformer display for some shallow-water data taken north of the island of Elba off the Italian coast. Note the large amount of clutter on the beamformer display, much of which is attributable to bathymetric features.

The poor performance of standard active sonars in the presence of reverberation is due to the suboptimum properties of delay-sum beamforming and matched-filter processing. It is well known that delay-sum beamforming and matched-filtering are optimum only for detecting and localizing a single-point scatterer in white gaussian noise. When closely spaced (by closely spaced, we mean relative to the main lobe width of the beam pattern and autocorrelation function of the matched-filter) or spread reverberators and/or colored interference are present, the delay-sum beamformer and matched-filter has poor detection performance and resolvability, that is, scatterers are not resolved. This is because the resolvability of delay-sum beamforming is limited by the main lobe width of the beam pattern (similarily for the matched-filter). Furthermore, even when reverberators are far apart, sidelobe leakage can be a significant problem.

The implementation of the optimum detector or estimator (e.g., likelihood-ratio test) requires the spatial-temporal statistical properties of the reverberation, ambient noise, and target acoustic pressure fields. However in practice, sufficient information is generally not available to implement the optimum receiver. For example, the pertinent ocean-acoustic parameters (e.g., bathymetry) are often inaccurate and are known only at isolated points. Furthermore, high numerical complexity is required to precisely model the underlying scattering and propagation physics. Thus it is not feasible to implement the optimum receiver.

An alternative methodology is *matched-field processing* (MFP) [1] where one fits the received data using the predicted acoustic pressure calculated via a numerical scattering-propagation model over the hypothesized target locations and all unknown/uncertain parameters, e.g., reverberators, bathymetry, geoacoustic parame-

ters, SVPs, target scattering functions, etc. The difficulty with this approach is the very large dimensionality of the search space to account for all the uncertainty and as before, the high numerical complexity to precisely model the underlying scattering and propagation physics.

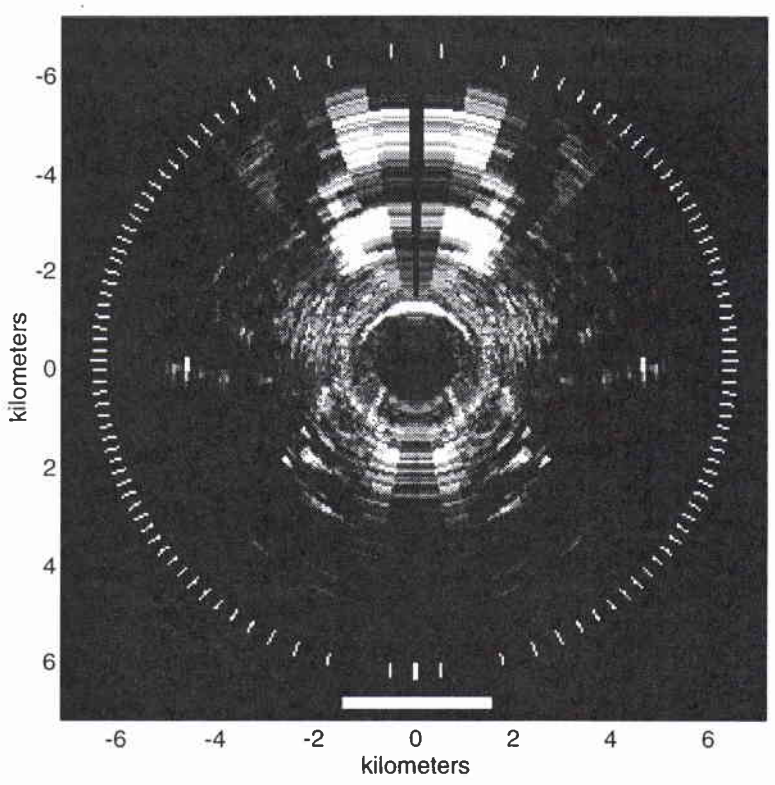

Figure 1 *An example of reverberation observed after a single ping using a 375–425 Hz HFM waveform. The display is showing the output of the beamformer after match-filtering. Note that 'light' intensities on the display mean stong returns and 'dark' intensities mean weak returns. This data was collected in about 120 m of water north of the island of Elba off the coast of Italy.*

It is conjectured that there is sufficient information available about the scattering mechanisms and acoustic environment to provide at least useful insight for modeling and suppressing reverberation components. We therefore propose a methodology in which efficient adaptive detection and localization algorithms are developed using acoustic propagation and scattering physics as a *guide* to determine simpler representations for the received data, for which the criteria is applicability of efficient adaptive signal-processing algorithms for the particular data structure. The objective is to (1) seek a data representation whose fundamental structure is approximately invariant to the uncertain acoustic parameters, and (2) allows development of computationally practical adaptive detection and localization algorithms. It is

necessary for the algorithms to be adaptive in order to compensate for the uncertainty in the acoustic environment. By invariant data structure we mean that the parametric representation does not change much due to small changes in the acoustic parameters. For example, if the observed data can be represented by a sum of sinusoids, then we desire that only the frequency and amplitudes vary as a function of the uncertain acoustic parameters, not the sinusoidal representation itself. Essentially, the idea is to embed the uncertain acoustic parameters in terms of the parameters of the simpler data structure, here the amplitudes and frequencies.

We now illustrate the concept using the following example. Consider the case of high-frequency acoustic propagation in deep water when the sound-velocity profile (SVP) is not precisely known. It is well known that the received data in deep water can be modeled as a superposition of delayed and attenuated versions of the transmitted signal, i.e., propagation via discrete multipaths. The uncertainty of the SVP is implicitly embedded in the multipath structure, that is, number of paths, arrival times and attenuations. Note that the basic multipath structure is approximately invariant to the SVP. Therefore the approach in this example is to develop algorithms which exploit the underlying discrete multipath structure and incorporating uncertainty in the arrival times, attenuations, and number of paths. We now discuss the special characteristics of shallow-water reverberation and related detection/localization issues.

The characteristics of reverberation are determined by the following three factors [2]: The first is propagation from the source to the reverberator, the second is the scattering process and the third is the propagation to the receiver. In shallow water the propagation processes have significant effect on the characteristics of shallow-water reverberation. For a discussion on deep- and shallow-water propagation the reader is refered to Jensen [1]. Some of the important issues regarding shallow-water propagation/reverberation in terms of how they affect detection/localization are the following:

1. The propagation and backscattering can have significant temporal spreading (i.e., greater than the spatial extent of the scatterer). For example, at a range of 13 km 2-way parabolic equation (PE) code [3] predicts that the backscattering from a 5×5 m square block lying on the ocean bottom in the Elba area will be spread nearly 0.4 s (see Fig. 2).
2. Empirical results suggest that propagation is often via a *continuum* of paths.
3. Because of temporal spreading, weak targets even at a considerable distance from the reverberator can be masked by temporally spread reverberation components. Furthermore, the echo from a point-like target can look similar to that from a reverberator, making classification difficult.

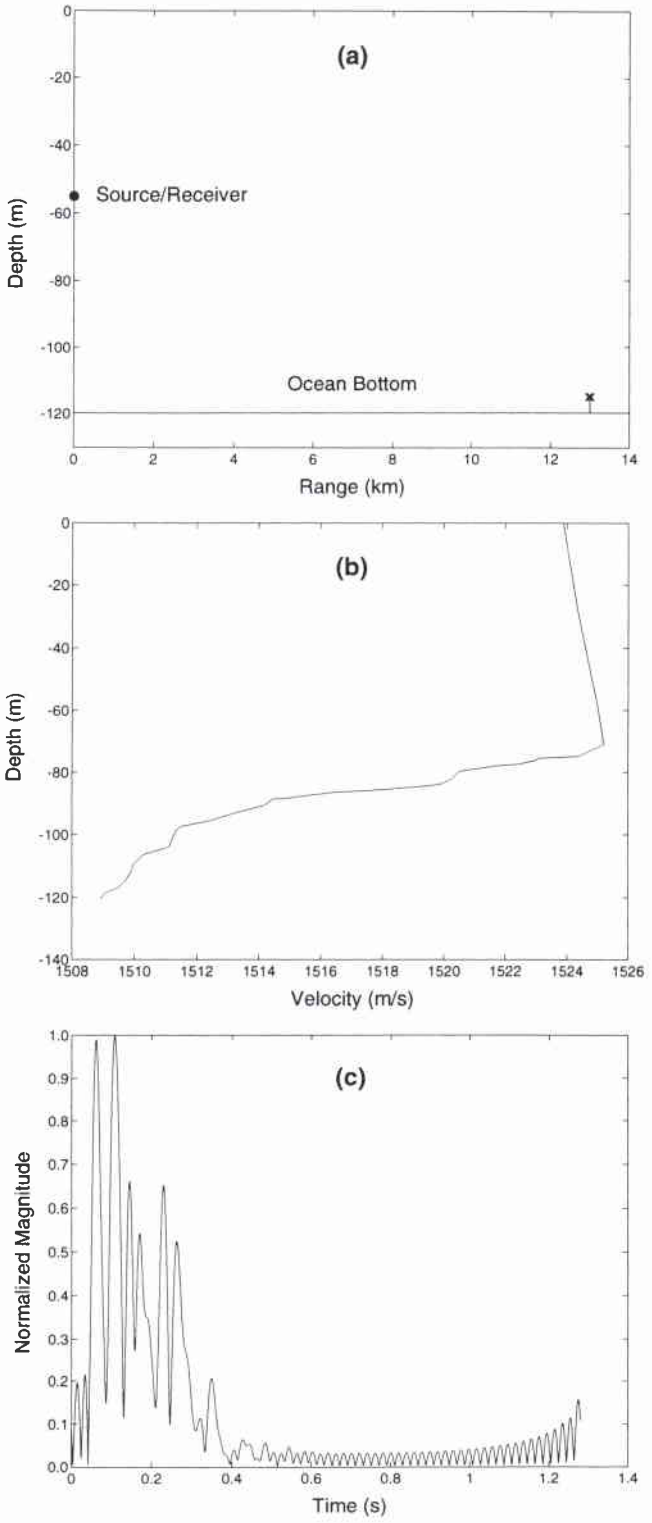

Figure 2 *Calculated backscatter from a discontinuity at 13 km for a 375–425 Hz bandpass pulse excitation. The acoustic parameters were chosen to correspond to realistic Elba Island area conditions. (a) The geometry used for the calculation. Note that the* 5×5 *m discontinuity is denoted by a cross. (b) Measured sound velocity profile used in calculation. (c) Calculated normalized backscattering. Note that spreading of 0.4 s corresponds to about 300 m in range.*

In this memorandum we apply the previously discussed methodology to develop algorithms for detecting and localizing targets in the presence of temporally spread reverberation components. The methodology is demonstrated by proposing that temporally spread reverberation components, spread either due to the medium and/or extended scatterers, can be accurately modeled using a reduced-rank representation [4] and expansion by discrete prolate spheroidal sequences. These representations lead to simple and efficient algorithms for reverberation suppression and target localization.

This memorandum is a compilation of three conference papers in which the results of this research were presented. The three papers present the derivation of the above reverberation representations, algorithms, and performance analysis. We now briefly summarize each.

In the first paper (Annex I) we show that a reduced-rank model is a simple, but accurate representation for temporally spread reverberation components. We then apply the Principal Component Inverse (PCI) method [5] to separate weak target components from overlapping strong reverberation components. Using both simulated data and real reverberation data, it is shown that the PCI method performs well. This work was presented and published at the *Low Frequency Active Sonar Conference*, SACLANT Undersea Research Centre, La Spezia, Italy, May 1993.

In the second paper (Annex II) we consider the problem of estimating arrival times of overlapping, temporally spread, multiple reverberation and target echoes which have propagated via an unknown channel. The temporal spreading is included in the model by using a discrete prolate spheroidal sequence expansion to represent the channel impulse response of given duration, but unknown shape. The unknown arrival times are estimated using an iterative approach which decomposes the original data into their constituent components and then estimates the arrival times through a sequence of one dimensional searches. Computer simulation examples indicate the method performs well. This work was presented and published at the *Seventh SP Workshop on Statistical Signal and Array Processing*, Quebec City, QC, Canada, June 1994 and is a collaborative effort with Geoff Edelson at Lockheed-Sanders Inc., Nashua, NH, USA. Parts of this work and related topics were also presented at the *GRETSI Conference*, Juan-Les-Pins, France, September 1993 and at the *IEEE Workshop on Underwater Acoustic Signal Processing*, Alton-Jone Campus, University of Rhode Island, Rhode Island, October 1993.

The third paper (Annex III) presents a theoretical performance analysis of the reduced-rank generalized likelihood ratio test (RR-GLRT) proposed for extending the PCI method to non-weak signal cases. In Fig. 3, we present some ROC curves (obtained via computer simulation) which show the dramatic improvement of the RR-GLRT over conventional matched-filtering. For a discussion on how to apply the RR-GLRT and detection in reverberation, the reader is referred to Appendix A. This work was motivated by the success of the PCI method for suppressing strong, temporally spread reverberation components in Annex I. The objective of the RR-GLRT

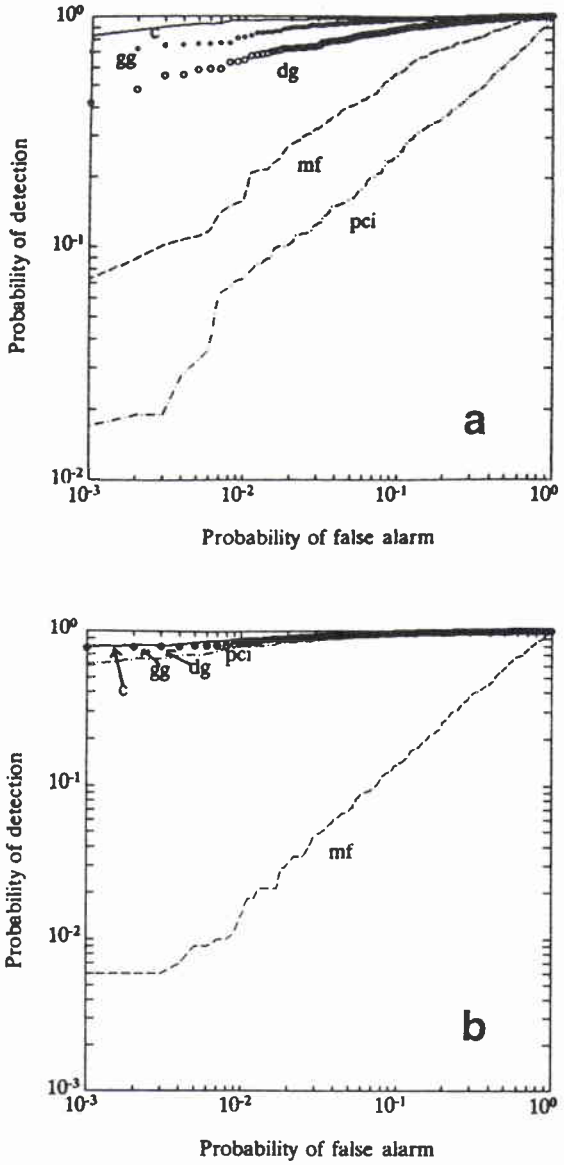

Figure 3 *Measured receiver operating characteristic curves for a 20 element equi-spaced line array used to detect a narrowband signal arriving at broadside in the presence of interference from two narrowband jammers plus white Gaussian noise: (a) strong signal case where the signal strength is −5 dB below the interference; (b) weak signal case where the signal strength is −15 dB below the interference. The jammers are located in spatial frequency half a DFT bin-width about broadside and a total of 20 independent data snapshots are used. (Notation: c – clairvoyant detector; gg – Gaussian RR-GLRT; dg – deterministic RR-GLRT; mf – matched-filter; pci - PCI method.)*

analysis is to have formulas available to determine the applicability and performance of the RR-GLRT for suppressing reveberation components which can be represented by a reduced-rank model and when the signal is not weak. The performance analysis shows that the RR-GLRT is closely related to the optimum Gauss-Gauss receiver. This work was presented and published at the *VII European Signal Processing Conference*, University of Edinburgh, Scotland, UK.

2 Conclusions

This memorandum is the first in the series of two documents on reverberation suppression. The objective of this memorandum was to lay a theoretical foundation for the proposed reverberation suppression methodology and techniques. The second follow-up document will focus on the application of these techniques to actual shallow-water reverberation data from the Elba area collected during November 1994. In particular, the second document will present experimental examples using reverberation from known bottom features to show that the proposed methodology and techniques can result in significant performance gains over standard delay-sum beamforming and matched-filtering. Also, aspects regarding the practical implementation of these techniques on real sonar data will be discussed.

We now summarize the key results presented here and also discuss some issues and questions raised by this work. We have proposed a signal-processing methodology in which reverberation suppression algorithms are developed by using acoustic propagation and scattering physics as a *guide* to modeling and determining simpler representations for the received data (i.e., reverberation and target waveforms), for which the criteria is applicability or development of efficient adaptive algorithms. The philosophy used here is that it is important to utilize as much prior propagation and scattering information as is practical to improve performance and also use the predicted waveform structures to justify the algorithms being used. This methodology was demonstrated by showing that temporally spread reverberation components, spread either due to the medium and/or extended scatterers, can be accurately modeled using a reduced-rank representation and expansion by discrete prolate spheroidal sequences. These representations lead to simple and efficient algorithms (which are presented in the three papers in the Annexes) for reverberation suppression and target localization. Theoretical analysis and computer simulation results indicate that these algorithms perform well.

An important advantage of this approach is that prior environmental information can be utilized in a computationally efficient manner while at the same time adaptively compensating for uncertainty in the environmental information. This is in contrast to a standard matched-field processing approach where the uncertainty in environmental information would have to be compensated by possibly a very high order multidimensional search. Thus the proposed approach is particularily useful in shallow water where acoustic propagation has considerable interaction with the ocean bottom, but the prior bathymetry information can be limited, e.g., bathymetry and sediment properties are coarsely sampled.

One potential scenario envisioned for application of these techniques is where a hostile submarine is stalking a strait or harbor entrance and exploits reverberation from bottom features (e.g., shoals, trenches, cliffs, etc.) to avoid detection. To illustrate how easy it would be for an adversary to avoid detection, consider a realistic example where the beamwidth of the delay-sum beamformer is 4 degrees. At a range of 15 km, this translates to a cross-range resolution of about 1 km. Thus a weak and slow-moving target would be masked by the main beam response of the reverberator at any distance less than 1 km in cross-range. Therefore, an intelligent adversary could easily avoid detection if conventional processing is used.

For example, to apply the proposed methodology, information from historical bathymetric data bases in conjunction with numerical scattering models and augmented on online reverberation measurements would be used to determine areas of strong reverberation that a target could hide in. This analysis is then used to design and choose the reverberation suppression algorithms for a particular area; e.g., near a distinct shoal, one of the data adaptive high resolution algorithms proposed in this memorandum could be used; on the other hand, if the bathymetry is 'flat', then delay-sum beamforming followed by matched-filtering might be sufficient.

Future work will consider the application of more sophisticated propagation and scattering models for developing reverberation suppression algorithms using the methodology outlined earlier. One potential direction of study is the utilization of more detailed channel propagation and scattering prior information in the reduced-rank generalized likelihood-ratio tests.

Another area for future work is automating the application of the proposed algorithms (e.g., algorithm determination, parameter setting, thresholding etc.). It is envisioned that a sonar system would have an intelligent, automated front-end (e.g., expert system) which would take as its inputs information from bathymetric data bases, environmental information, numerical scattering models, and observed reverberation and noise data. The front end would then automatically decide which detection/localization algorithms to use and set algorithm parameters and thresholds.

References

[1] Jensen, F.B., Kuperman, W.B., Porter, M.B. and Schmidt, H. *eds.* Computational Ocean Acoustics. New York, NY, American Institute of Physics, 1994. [ISBN 1-56396-209-8]

[2] Schmidt, H. Numerical modeling of three-dimensional reverberation from bottom facets. *In:* Ellis, D.D., Preston, J.R. and Urban, H.G., *eds.* Ocean Reverberation. Dordrecht, the Netherlands, Kluwer, 1993: pp. 105–112. [ISBN 0-7923-2420-X]

[3] Collins, M.D. and Evans, R.B. A two-way parabolic equation for acoustic backscattering in the ocean. *Journal of the Acoustical Society of America*, **91**, 1992: 1357–1368.

[4] Scharf, L.L. The SVD and reduced rank signal processing. *Signal Processing*, **25**, 1991: 113–133.

[5] Kirsteins, I.P. and Tufts, D.W. Adaptive detection using low rank approximation to a data matrix. *IEEE Transactions on Aerospace and Electronic Systems*, **30**, 1994: 55–67.

Appendix A

Detection in reverberation using the RR-GLRT

The RR-GLRT can be applied to any situation where the reverberation and target echo components can be represented using a reduced-rank model. We now propose an approach using the reduced rank representation from Annex I.

First, recall that the observed data matrices in the RR-GLRT are assumed to be of the form (see Annex III)

$$X = \mathcal{H}_r + N \quad \text{(noise only)}, \tag{A1}$$

or

$$X = \mathcal{H}_r + SC + N \quad \text{(signal plus noise)}, \tag{A2}$$

where $\mathcal{H}_r$ is the low rank interference component due to the temporally spread reverberation (see Annex I) and SC is the target echo component to be detected. The target component is written as the product of matrices S and C. The columns of S generate the target echo subspace and the elements of C are the expansion coefficients. Note that the target echo component in the kth column of the data matrix X is written as

$$\mathbf{e}_k = \sum_{n=1}^{M} c_n^k \mathbf{s}_n, \tag{A3}$$

where the $\{\mathbf{s}_k\}$ are the basis vectors which generate the target echo component and the $\{c_n^k\}$ are the scale factors. We now show that (A3) can be used to represent temporally spread target echos.

From Annex I formulas (9) and (12), the observed data matrix is

$$\mathcal{H} = \begin{bmatrix} \tilde{G}_{L-1} & \tilde{G}_{L-2} & \cdots & \tilde{G}_0 \\ \tilde{G}_L & \tilde{G}_{L-1} & \cdots & \tilde{G}_1 \\ \vdots & \vdots & \cdots & \vdots \\ \tilde{G}_{N-1} & \tilde{G}_{N-2} & \cdots & \tilde{G}_{N-L} \\ \overline{\tilde{G}}_0 & \overline{\tilde{G}}_1 & \cdots & \overline{\tilde{G}}_{L-1} \\ \overline{\tilde{G}}_1 & \overline{\tilde{G}}_2 & \cdots & \overline{\tilde{G}}_L \\ \vdots & \vdots & \cdots & \vdots \\ \overline{\tilde{G}}_{N-L} & \overline{\tilde{G}}_{N-L+1} & \cdots & \overline{\tilde{G}}_{N-1} \end{bmatrix} \tag{A4}$$

Letting $X = \mathcal{H}^T$, we see that each row of X has the form

$$\mathbf{x}_k = [\tilde{G}_{L+k-1}\tilde{G}_{L+k-2}\ldots\tilde{G}_k]^T \tag{A5}$$

We can now apply the same arguments of Annexes I and II and propose that temporally spread target echo components in each column of X can be accurately represented using a discrete prolate spheroidal sequence expansion, that is, the $\{\mathbf{s}_k\}$ in formula (A3) are the discrete prolate spheroidal sequences. The reader is referred to Annex II for details how to design the DPSSs.

Annex I

Model-aided data adaptive suppression of reverberation

The paper reproduced in this annex was originally published as:

Kirsteins, I.P. (1993). Model-aided data adaptive suppression of reverberation. *In*: Weatherburn, R. and Murdoch, G. *eds*., Low frequency active sonar. A NATO conference held by SACLANTCEN on 24–28 May, 1993, collection of unclassified papers, Vol. 1, SACLANTCEN CP-42. La Spezia, Italy, NATO SACLANT Undersea Research Centre: pp: C/11-1 to C/11-12. [AD B 182 781]

intentionally blank page

Report no. changed (Mar 2006): SM-287-UU

SACLANTCEN CP-42

MODEL-AIDED DATA ADAPTIVE SUPPRESSION OF REVERBERATION

I.P. Kirsteins
SACLANT Undersea Research Centre, Viale San Bartolomeo 400, 19138 La Spezia (SP), Italy

Abstract We propose a processing methodology which is based on the piece-wise modeling, adaptive estimation, and removal of reverberation components. An important feature of this approach is that backscatter models and information from pre-processing are used to guide the modeling of the reverberation components and the design of the algorithms to estimate them. The proposed processing methodology is developed for the case when strong, highly temporally localized reverberation components plus a weak target echo are present in single channel time series data and the only prior information available about the reverberator is the approximate location and extent. For this case we derive a reverberation suppression algorithm which is based on the reduced-rank modeling of the reverberator transfer function followed by application of the Principal Component Inverse (PCI) method of reduced-rank adaptive interference cancellation. The algorithm is tested using simulated and real reverberation data.

1. Introduction

An important problem in active sonar is the detection of targets in the presence of bottom and surface reverberation. It is well known that active sonars using standard delay-sum beamforming and matched filtering perform poorly in the presence of strong reverberation. This performance loss generally arises from the suboptimum properties of standard sonar signal processing when strong 'signal-like' reverberation components are present (delay-sum beamforming and matched filtering are optimum only for detecting and localizing a single point scatterer in white gaussian noise). These 'signal-like' components arise from abrupt changes in ocean boundaries (e.g., cliffs, trenches, pinnacles, seamounts, facet-like surface waves etc.) [1]. The poor performance leads to masking of targets and high false alarm rates.

The design of an optimum receiver (e.g., likelihood-ratio test) requires the spatial-temporal statistical properties of the reverberation, ambient noise, and target acoustic pressure fields. Conceptually, the statistical properties of the acoustic back-scattered field are predictable if all the pertinent scattering physics, propagation physics, and ocean-acoustic parameters (ocean surface, bathymetry, water column properties etc.) were known. The difficulty in practice is that excessive complexity is required to exactly model the acoustic backscattering and propagation. An equally important problem is that the available

bathymetric/environmental data is often incomplete and known with limited accuracy. For example, the sound velocity profile and geo-acoustic parameters are usually measured at a small number of locations. In addition, bathymetric surveys may miss small-scale bottom features which can be important reverberators. Hence the optimum receiver can not be implemented. However, it is conjectured that sufficient information is available about the scattering mechanisms, bathymetry, and ocean environment to provide useful predictions to aid in modeling and suppressing the reverberation components. For example, at least the 'coarse' reverberation structure (e.g., location, energy distribution and extent) should be predictable using acoustic backscattering models such as the two-way PE method [2] or *BISSM2* [3] in conjuction with bathymetric and environmental data bases.

The methodology that we propose for processing the reverberation data is to identify, categorize, model, and remove the reverberation components in a piece-wise fashion based on their ease of separability from the ambient noise and target signals. The modeling and estimation of the reverberation components are guided by backscatter model predictions and preliminary analysis of the data, such as standard beamforming and matched filtering. In essence, the estimation step is used to compensate for the uncertainty in the backscatter predictions.

This piece-wise approach to modeling and processing complicated data is similar to that proposed by Kirsteins and Tufts [4] for processing Arctic sea noise data and also by Middleton [5] for strong non-gaussian interference. Middleton proposed that one way of dealing with non-gaussian interference is to estimate and then subtract out the strong non-gaussian interference prior to signal processing and reduce the problem to one of processing in ambient noise [5]. The above methodology is also closely related to the residual signal analysis scheme of Costas [6] In [6] Costas considers the problem of recovering the individual signals that the received waveform is composed of, that is, the received waveform consists of a sum of several signals plus ambient noise and the problem is to estimate each of the signal components. He proposes a cooperative arrangement between estimation processors in which each processor acts as an adaptive interference canceller for all the other processors while estimating its own signal [6].

In this paper we develop the methodology for the case when strong, 'signal-like' or temporally localized reverberators plus a weak target echo are present in single channel time series data and the only prior information available about the reverberator is the approximate location and duration (see Figure 1). For this case we derive a novel algorithm for estimating and removing the strong, temporally localized reverberators. The algorithm is based on the reduced-rank modeling of the measured reverberator transfer function followed by application of the PCI method [8–12]. of reduced-rank interference cancellation.

The rest of the paper is organized as follows: In the next section we derive the reduced-rank reverberation suppression algorithm. We then present some simulated and real reverberation data examples in Section 3, and in Section 4 concluding remarks.

2. Reduced-Rank Estimation and Removal of Temporally Localized Reverberators

In this section we motivate the use of a reduced-rank model to represent the measured reverberator and ocean-acoustic channel transfer function, and then derive the reduced-rank reverberation suppression algorithm for the single channel case e.g., beam outputs or individual hydrophones. For a review and discussion on reduced-rank modeling the reader is referred to [15,16].

The observed reverberation plus target time series, denoted as $d(t)$, can be written as

$$d(t) = h(t) * s(t) + T(t) * s(t) + n(t), \tag{1}$$

where the operator '$*$' denotes convolution, $h(t)$ is the combined impulse response of the reverberator(s) and ocean-acoustic channel, $T(t)$ is the combined impulse response of the target and ocean-acoustic channel, $s(t)$ is the transmitted signal, and $n(t)$ is some noise component (e.g., ambient noise). In the frequency domain the first convolution in (1) is

$$D(w) = H(w)\, S(w), \tag{2}$$

where $D(w)$, $H(w)$, and $S(w)$ are the Fourier transforms of $d(t)$, $h(t)$, and $s(t)$ respectively. Typically $S(w)$ is restricted to some band, say between w_1 and w_2. Therefore we consider $H(w)$ only in the interval $[w_1, w_2]$. Next sample $H(w)$ to form the discrete sequence

$$H_n = H(w_1 + \Delta w n), \qquad n = 0, 1, \ldots N-1, \tag{3}$$

where $w_2 = w_1 + \Delta w(N-1)$.

Let us now assume that only one strong, temporally localized reverberation component is present in $d(t)$ (1). More precisely, by temporally localized reverberation component we mean that most of the energy of the combined reverberator and ocean-acoustic channel impulse response is concentrated in a small time interval (e.g., features A and B in Figure 1). We now argue that the sequence $\{H_n\}$ can be approximated using a reduced-rank model when $h(t)$ is temporally localized. Our argument starts with the observation that since $h(t)$ can be expressed as

$$h(t) = \frac{1}{\pi} \int H(w) e^{iwt}\, \mathrm{d}w, \tag{4}$$

it can be regarded as a 'Fourier transform' of the 'waveform' $H(w)$ ($h(t)$ is the complex conjugate of the Fourier transform of $(1/2\pi)\overline{H}(w)$). If $h(t)$ is concentrated in some time interval $[\tau_1, \tau_2]$, we can then say that the 'waveform' $H(w)$ is approximately bandlimited. It is well known that a segment of N samples from a bandpass stationary random process with a rectangular power spectrum of bandwidth β and sampled at rate f_s can be accurately approximated using a linear expansion of only $(2\beta/f_s)N$ discrete prolate spheroidal sequences (DPSS) [16]. Hence from the above discussion, we infer that the data vector

$$\mathbf{h} = [H_0 H_1 \cdots H_{N-1}]^T \tag{5}$$

should roughly be representable using a linear expansion of about r terms where,

$$r = \frac{(\tau_2 - \tau_1)}{f_s} N \tag{6}$$

and $f_s = 1/\Delta w$. Formula (6) can be simplified by noting that as $\Delta w \to 0$, it tends to

$$r = (\tau_2 - \tau_1)(w_2 - w_1) \tag{7}$$

recalling that $[w_1, w_2]$ is the signal band. It is emphasized that formula (7) is exact only for a bandpass stationary random process with a rectangular spectrum. In general it should only be used as a heuristic rule or bound to gain rough insight into the dimensionality of $H(w)$. The actual dimensionality will vary depending on the shape of $h(t)$.

We say that **h** is low rank when the dimensionality of **h** is much less than the dimensionality of the background noise (e.g., rank of noise covariance matrix) [15,16]. Therefore, **h** is expected to be low rank when $(\tau_2 - \tau_1)(w_2 - w_1) << N$ and the background noise is full rank (e.g., white noise). Thus the PCI method [8–12] can be used to remove temporally localized reverberators. A detailed review of the PCI method is provided in Appendix A.

First some preliminaries before presenting the reverberation suppression algorithm. The signal spectrum $S(w)$ within the band of interest $[w_1, w_2]$ is assumed to be non-zero everywhere and with no deep notches. The need for this will be seen later in the algorithm steps. Secondly, the target echo is assumed to be much weaker than the reverberator and the regions where strong, temporally localized reverberation components are present have been identified. The target echo is required to be weak to minimize the influence of the signal when estimating the reverberation component. We now give the steps of the reverberation suppression algorithm:

1. **Fourier transform the data**

$$\tilde{D}_k(w) = \int_{T_1^k}^{T_2^k} d(t) e^{-iwt}\, dt, \tag{8}$$

where the interval $[T_1^k, T_2^k]$ encompasses the kth reverberation component in formula (1). The interval $[T_1^k, T_2^k]$ is determined from backscatter models and/or preliminary analysis of the data, e.g., matched filtering.

2. **Measurement of reverberator-channel and target transfer function**

Calculate

$$\tilde{G}_n^k = \frac{\tilde{D}_k(w_1 + \Delta w n)}{S(w_1 + \Delta w n)}, \qquad n = 0, 1, \ldots N-1, \tag{9}$$

It is important that $S(w)$ has no deep notches within $[w_1, w_2]$. The effect of deep notches is to enhance any noise components which may be present in $\tilde{D}_k(w)$.

3. **Apply PCI method to remove reverberation component**

The steps of the PCI method presented in Appendix A are applied to the sequence $\{\tilde{G}_n^k\}$ (9) to estimate the reverberator response H_n and then subtract it from $\{\tilde{G}_n^k\}$. The residual contains an estimate of the target response and background noise.

Formula (7) can be used to gain insight into the rank of the interference. The rank of the interference is more precisely determined by computing the singular value decomposition of the data matrix and then finding the number of dominant singular values (see Appendix A).

Discussion It is pointed out that the only prior information necessary to implement the algorithm is the approximate location and duration of the reverberator-channel response. This can be determined from preliminary analysis of the data or backscatter models. No information regarding the shape of the reverberator-channel response is needed.

Tufts et al. [7] also proposed using the PCI method to suppress reverberation. In [7] the PCI method is applied directly to the reverberation time series data. The new approach presented here applies the PCI method to the measured reverberator-channel transfer function and only requires that the reverberator-channel impulse response is temporally localized. It does not require that the reverberation time series possess any low rank properties.

The steps of the proposed processing methodology are now summarized. They are as follows:

1. Identify and locate the regions where strong, temporally localized reverberators are present using preliminary analysis, e.g., standard beamforming and matched filtering, and backscatter model reverberation level predictions. The validity of the reduced-rank model for the reverberator-channel transfer function is determined using formula (7) and from the number of dominant singular values the data matrix has (see Appendix A).
2. Estimate and remove the strong, temporally localized reverberators using the PCI method.
3. Perform target detection/localization on the residual data.

3. Experimental Results

We now present some simulated and real data examples. We start by giving an example to show how the low rank structure of the PCI method data matrix (12) can arise.

Low Rank Data Matrix Suppose our received waveform is

$$d(t) = \alpha_1 s(t - \tau_1) + \alpha_2 s(t - \tau_2), \tag{10}$$

for example, arising from two point scatterers over direct path propagation. It can then be shown that

$$H(w) = \alpha_1 e^{-i\tau_1 w} + \alpha_2 e^{-i\tau_2 w}. \tag{11}$$

If we sample (11) over some interval and arrange the samples into the matrix given by formula (12), it is easy to show the data matrix is rank 2 (e.g., every row of the data matrix is some linear combination of the same two discrete exponential sequences).

Computer Generated Data Next we present a computer generated example where a weak target echo is recovered in the presence of a strong, highly temporally localized reverberator plus white Gaussian noise. The bandwidth of the reverberator is chosen to be 0.0488 Hz and the sampling rate is 1 Hz. The envelopes of the entire observed impulse response (reverberator, target and noise) and the target echo are plotted in Figure 2a. Note that the signal has been deconvolved from the data. The PCI method using a rank of 5 is applied to remove the reverberator and the residual is plotted in Figure 2b. Note that the target echo is distinctly observable in the residual.

Real Reverberation We now apply the algorithm to some real shallow water reverberation data. The data was collected in area where the average depth was about 110 m. The reverberation data used in this example is the output basebanded time series from a single beam. The transmitted waveform is a 375–395 Hz HFM pulse of 2.45 s duration. In Figure 3 the envelope of the matched filter output for a single beam is plotted. It can be seen that there are several distinct peaks present in the matched filter output, particularly the feature labeled 'A'. We now use the PCI method to estimate and remove the reverberation component corresponding to peak 'A'.

To apply the algorithm, a 5.3 s segment of data about the reverberator was taken and its Fourier transform evaluated at 100 equi-spaced points in the interval 375–395 Hz. The measured impulse response after the signal has been deconvolved from the data is plotted in Figure 4 (see step 2 of algorithm). Insight into the rank of the reverberator can now be determined using the measured reverberator response (Figure 4) to estimate the reverberator duration ($\sim$ 0.4 s) and then substituting it into formula (7), obtaining $r = 8$ ($= 0.4 \times 20$). The data matrix (see step 3 of algorithm) had actually 4 dominant singular values so a rank of 4 was used to implement the PCI method. The estimated reverberator and residual impulse response are plotted in Figures 5 and 6. It can be seen from Figure 6 that the reverberator has been accurately removed.

4. Conclusion

A new algorithm has been presented for suppressing strong, temporally localized reverberation components. The only prior information the algorithm requires is the approximate location and duration of the reverberation component. This can be obtained from preliminary analysis, e.g., beamforming and matched filtering or backscatter model predictions. Future work includes extending the algorithm to the strong target echo case and performance analysis.

Acknowledgement The author would like to thank Dale Ellis and Reginald Hollett for providing the reverberation data set and also the many helpful discussions.

A. Review of PCI Method

The PCI method [8–12] of adaptive interference cancellation and detection is based on reduced-rank nulling of interference. The PCI method exploits the low rank structure of the data covariance matrix or equivalently, of the data matrix. An important advantage of the PCI method over conventional methods such as adaptive control loops and the Sample Matrix Inverse method is that it achieves a much more rapid rate of adaptation [8–12].

In the PCI method, the interference is first regarded as a 'signal' to be enhanced. Then reduced-rank signal enhancement [10,13,14] is applied to obtain an estimate of the interference. This interference is subtracted from the observed data and the residual is then processed to extract the desired signal information, e.g., presence of signal. The key idea in the signal enhancement algorithm [10,13,14] and the PCI method is to arrange the data samples in some matrix form which exploits the low rank structure of the data. More specifically, the steps for the time series version of the PCI method are as follows:

1. **Construction of Data Matrix**

   The data sequence $\{H_n\}_{n=0}^{N-1}$ is arranged into the forward-backward matrix

$$\mathcal{H} = \begin{bmatrix} H_{L-1} & H_{L-2} & \cdots & H_0 \\ H_L & H_{L-1} & \cdots & H_1 \\ \vdots & \vdots & & \vdots \\ H_{N-1} & H_{N-2} & \cdots & H_{N-L} \\ \overline{H}_0 & \overline{H}_1 & \cdots & \overline{H}_{L-1} \\ \overline{H}_1 & \overline{H}_2 & \cdots & \overline{H}_L \\ \vdots & \vdots & & \vdots \\ \overline{H}_{N-L} & \overline{H}_{N-L+1} & \cdots & \overline{H}_{N-1} \end{bmatrix}, \tag{12}$$

   where L is the number of columns and '$\overline{\ }$' denotes complex conjugate.

2. **Estimating the Interference Component**

   The interference waveform is estimated by arithmetically averaging all multiple occurences of each data sample in the low rank approximation to $\mathcal{H}$, denoted as $\mathcal{H}_r$, which is found as the solution to

$$\min_{\mathcal{H}_r \text{ subject to } \operatorname{rank}[\mathcal{H}_r] = r} \| \mathcal{H} - \mathcal{H}_r \|_F^2 . \tag{13}$$

The solution to (13) can be easily calculated using the singular value decomposition (SVD) of the data matrix $\mathcal{H}$. Also, the rank 'r' can be estimated by determining the number of dominant singular values present.

3. **Removing the Interference Component**

   The estimated interference waveform, denoted as $\tilde{H}_n$, is subtracted from the data:

$$R_n = H_n - \tilde{H}_n. \tag{14}$$

References

[1] Gerstoft, P. and Schmidt, H. A boundary element approach to ocean seismoacoustic facet reverberation, *Journal of the Acoustical Society of America*, **89**, 1991: 1629–1642.

[2] Collins, M.D. and Evans, R.B. A two-way parabolic equation for acoustic backscattering in the ocean, *Journal of the Acoustical Society of America*, **91**, 1992: 1357–1368.

[3] Caruthers, J.W., Sandy, R.J. and Novarini, J.C. Modified bistatic scattering strength model (BISSM2), NOARL SP 023:200:90. Stennis Space Center, NOARL, 1990.

[4] Kirsteins, I.P. and Tufts, D.W. Methods of computer-aided analysis of non-gaussian noise and application to robust adaptive detection, 1984. [AD A 148 879]

[5] Middleton, D. Multiple-element threshold signal detection of underwater acoustic signals in non-gaussian interference environments, NOSC CR 231, San Diego, CA NOSC, 1983. [AD A 140 620]

[6] Costas, J.P. Residual signal analysis, *Proceedings of the IEEE*, **68**, 1980: 1351–1352.

[7] Tufts, D.W., Kil, D.H. and Slater, R.R. Reverberation suppression and modeling, *In*: Urban, H.G., Ellis, D.D. and Preston, J.R, *eds*., Ocean Reverberation, a NATO symposium held at SACLANTCEN, 25–29 May, 1992. Dordrecht, Kluwer, 1993.

[8] Kirsteins, I.P. and Tufts, D.W. On the probability density of signal-to-noise ratio in an improved adaptive detector, *In*: Institute of Electrical and Electronics Engineers. Acoustics Signal Processing Society. ICASSP-85, IEEE International Conference on Acoustics, Speech, and Signal Processing, Tampa, Florida., 26–29 March 1985. Piscataway NJ, IEEE, 1985: pp. 572–575. [LCN 84-62724]

[9] Kirsteins, I.P. and Tufts, D.W. Rapidly adaptive nulling of interference. *In*: Bouvet, M. and Bienvenu, G., *eds*., High resolution methods in underwater acoustics. Berlin, Springer, 1991. [ISBN 3-540-53716-3]

[10] Kirsteins, I.P. and Tufts, D.W. Signal enhancement by low rank approximation to a data matrix with application to adaptive detection, *IEEE Transactions on Aerospace and Electronic Systems*, [to appear in 1994].

[11] Tufts, D.W. Kirsteins, I.P. and Kumaresan, R. Data-adaptive detection of a weak signal, single frequency, plane-wave signal in noise and strong, unidirectional interference, *In*: Wegman, E.J. and Smith, J.G., *eds*., *Statistical Signal Processing*. New York, NY, Marcel Dekker, 1984. [ISBN 0824771591]

[12] I.P. Kirsteins, Analysis of reduced-rank interference cancellation, PhD thesis, University of Rhode Island, Kingston, RI, 1991.

[13] Shah, A.A. and Tufts, D.W. Estimation of the signal component of a data vector, *In*: Institute of Electrical and Electronics Engineers. Signal Processing Society. ICASSP-92, IEEE International Conference on Acoustics, Speech, and Signal Processing, San Francisco, 23–26 March 1992. Piscataway, NJ, IEEE, 1992, volume 5, 393–396. [ISBN 0-7803-0533-7]

[14] Tufts, D.W. and Shah, A.A. , Blind Wiener filtering: Estimation of a random signal in noise using little prior knowledge, *In*: Institute of Electrical and Electronics Engineers. Signal Processing Society. ICASSP-93, IEEE International Conference on Acoustics, Speech, and Signal Processing, Mineapolis, MN, April 1993.

[15] Scharf, L.L. and Tufts, D.W. Rank reduction for modeling stationary signals, *IEEE Transactions on Acoustics, Speech and Signal Processing*, **35**, 350–354, 1987.

[16] Scharf, L.L. The SVD and reduced rank signal processing, *Signal Processing*, **25**, 1991: 113–133.

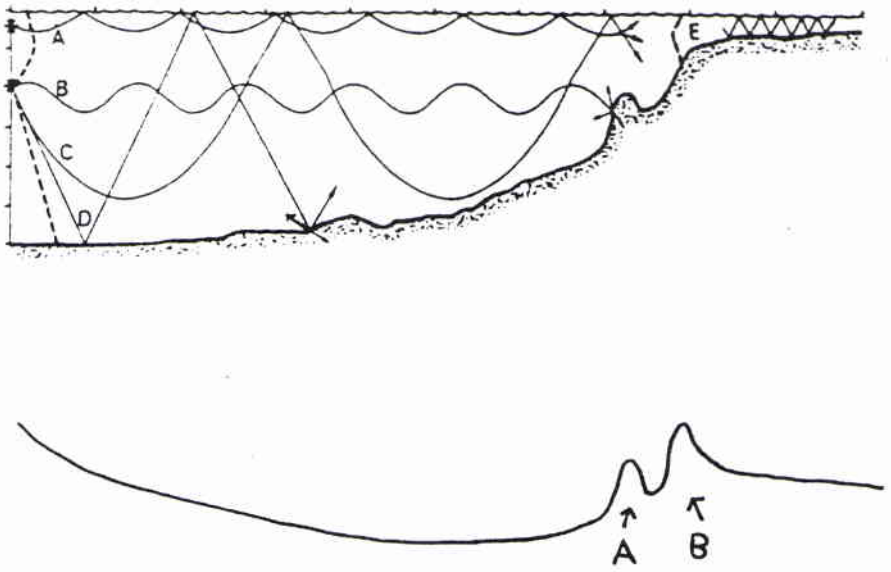

Figure 1. Example of prior information available.

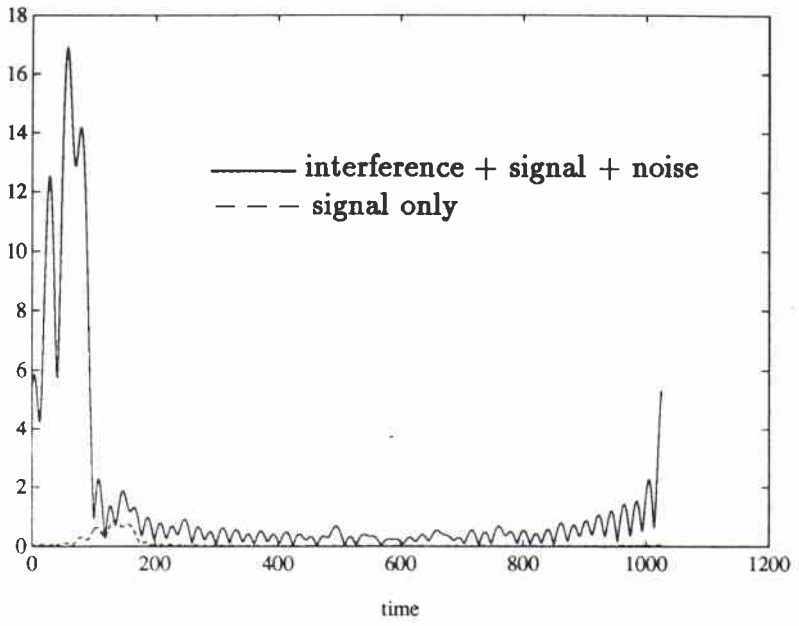

Fig. 2a) Interference, signal and noise impulse response.

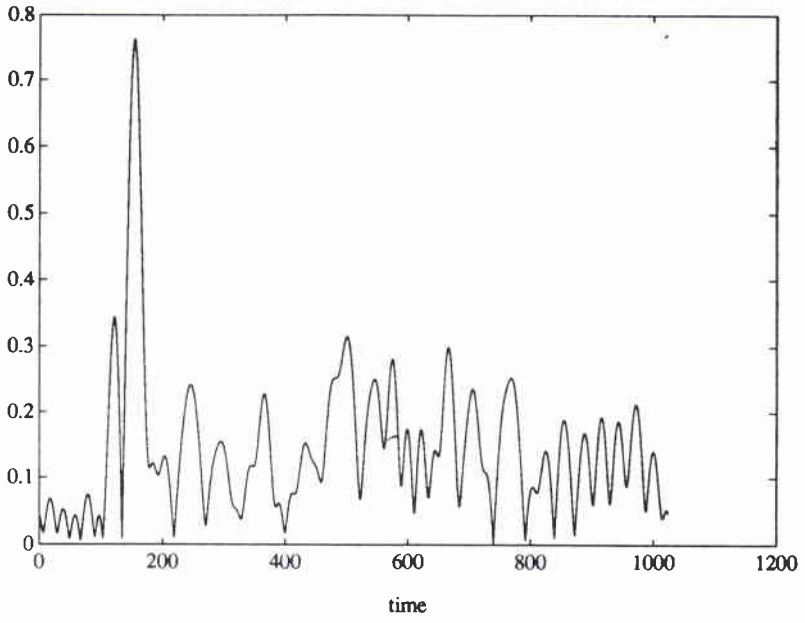

Fig. 2b) Residual impulse response after estimated interference has been subtracted.

Figure 2. Computer generated data example.

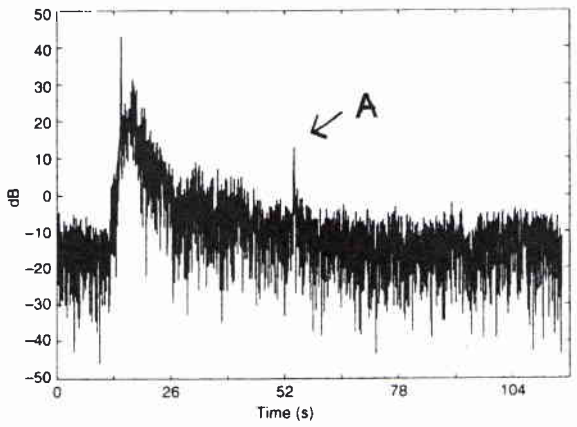

Figure 3. Single beam matched filter output.

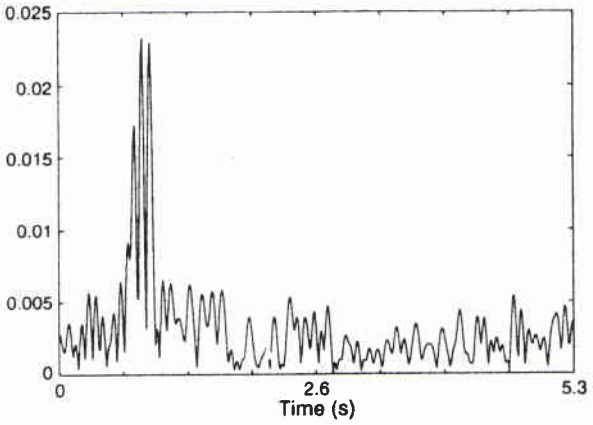

Figure 4. Measured impulse response of reverberator.

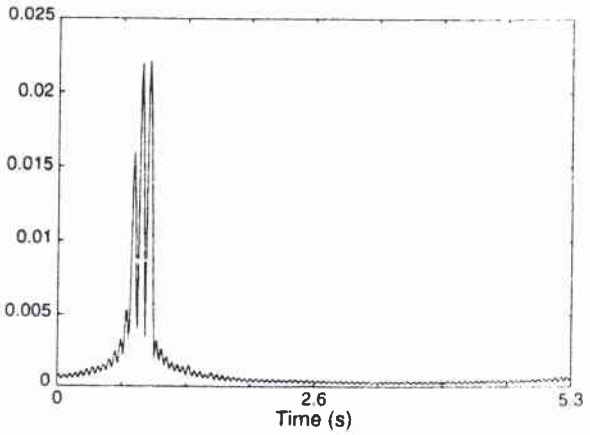

Figure 5. Estimated reverberator impulse response using reduced-rank signal enhancement.

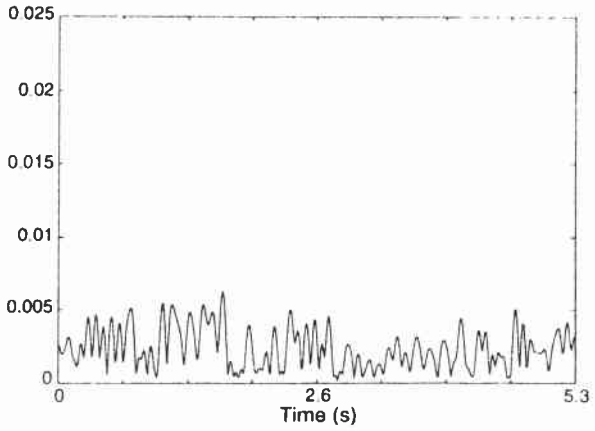

Figure 6. Residual impulse response after estimated reverberator component has been subtracted.

Annex II

Modeling and suppression of reverberation components

The paper reproduced in this annex was originally published as:

Edel, G.S. and Kirsteins, I.P. (1994). Modeling and suppression of reverberation components. *In*: Gingras, D., Fortier, P., Philibert, B. *eds*., Proceedings, IEEE seventh SP workshop on statistical signal and array processing, 26–29 June, 1994. Quebec, Universiteé Laval: pp. 437–440. [ISBN 2-9804169-0-8]

intentionally blank page

Modeling and Suppression of Reverberation Components

Geoffrey S. Edelson *Ivars P. Kirsteins*†

Lockheed Sanders, Inc., P.O. Box 868, Nashua, NH 03061-0868 USA

†SACLANT Undersea Research Centre, Viale San Bartolomeo 400, 1-19138 La Spezia, Italy

Abstract - **We propose a maximum likelihood type approach for estimating the arrival times of signals which have propagated via a continuum of paths, i.e. temporally spread channels. The channel spreading is included in the model by using a discrete prolate spheroidal sequence (DPSS) to represent the channel impulse response of given duration, but unknown shape. The unknown parameters are estimated using an iterative methodology which decomposes the original data into its constituent components and then estimates the parameters of the individual components through a sequence of one dimensional searches. Computer simulation examples indicate that the method performs well.**

I. INTRODUCTION

An important problem in active sonar is the detection and localization of targets in the presence of reverberation. Reverberation becomes particularly acute in shallow water due to the complex interaction of the reflectors with the channel. The reverberation plus target time series can be modeled as the joint convolution of the signal with the channel and scatterer impulse responses, that is,

$$d(t) = \underbrace{h_1(t-\tau_1)}_{\text{target}} * s(t) + \sum_{k=2}^{M} \underbrace{h_k(t-\tau_k)}_{\text{reverberation}} * s(t) + \underbrace{n(t)}_{\text{noise}} \quad (1)$$

where τ_k is the propagation delay, $h_k(t)$ is the path impulse response, and $s(t)$ is the transmitted signal. In many environments, the channel response $h_k(t)$ can not be adequately modeled as propagation over discrete paths. Rather, the propagation is via a *continuum* of paths and the spreading can be significantly greater than the spatial extent of the scatterer.

A standard approach for estimating the arrival times τ_k is to simply match filter the received data with the transmitted replica and then determine the location of the peaks in the matched filter output. However, the matched filter does not take channel spreading into account and the resolution of the matched filter is limited by the duration of the signal autocorrelation function. Equivalently, the resolution is proportional to the reciprocal of the signal bandwidth. Thus, in the presence of strong interference, weaker paths can be obscured or result in highly biased estimates. Recently, high resolution time of arrival estimation algorithms have been proposed [1, 2, 3, 4, 5]. However, they also assume that discrete propagation paths are present.

We propose a maximum likelihood type approach for estimating the arrival times which takes channel spreading into account. The approach is based on the frequency domain realization of the arrival time estimation [1, 2, 3] and then includes channel spreading by using a DPSS expansion to represent the channel response of given duration, but unknown shape. The unknown parameters are estimated using an iterative methodology [4, 5] which decomposes the original data into its constituent components and then estimates the parameters of the individual components through a sequence of one dimensional searches. We now derive the algorithm.

II. TIME OF ARRIVAL ESTIMATION

The objective is to estimate the τ_k from $d(t)$ in (1). Assuming the $h_k(t)$ are known, then the least-squares estimator (ML when $n(t)$ is white Gaussian) of the τ_k is [2]

$$\min_{\tau_1,\ldots,\tau_M} \int_{w_1}^{w_2} \left| D(w) - \sum_{k=1}^{M} e^{-i\tau_k w} H_k(w) S(w) \right|^2 \mathrm{d}w \quad (2)$$

where $D(w)$, $H_k(w)$, and $S(w)$ are the Fourier transforms of $d(t)$, $h_k(t)$, and $s(t)$ respectively. The interval $[w_1, w_2]$ is the signal frequency band in radians. Approximating the integral by a discrete sum, we get

$$\min_{\tau_1,\ldots,\tau_M} \sum_m |D(w_m) - \sum_{k=1}^{M} e^{-i\tau_k w_m} H_k(w_m) S(w_m)|^2 \quad (3)$$

where $w_m = w_1 + m\Delta w$ and Δw is the frequency sampling interval.

A problem in practice is that the shape of the $h_k(t)$ are usually not known. However, there are instances for which the extent or bound of the expected temporal spreading is known, i.e. the channel impulse response lies in $[-T_k, T_k]$. For example, the sound velocity profile and geoacoustic parameters are often known to sufficient accuracy to approximately predict or bound the channel spreading. Thus the $h_k(t)$ are also unknowns (where the extent of spreading is known, but the shape is not) along with the τ_k. Hence, the optimization of (3) has to be performed with respect to both the τ_k and the unknown $h_k(t)$ subject to the constraint that the non-zero response of $h_k(t)$ lies within some interval $[-T_k, T_k]$. This is a difficult optimization problem.

The approach we take is to approximately impose the constraint that $h_k(t)$ lies within $[-T_k, T_k]$ by expanding $H_k(w)$ using the DPSS's as basis functions. For an excellent review of the definition and properties of DPSS's, the reader is referred to [6]. Note that we will be using the same notation as in [6] for the DPSS's. We argue that

$$H_k(w_1 + m\Delta w) \approx \sum_{n=1}^{r_k} \alpha_n^k v_m^n(N, \beta_k) \qquad (4)$$

for $m = 1, 2, \ldots, N$ is a good approximation to $H_k(w)$ in the band $[w_1, w_2]$ where $r_k = T_k(w_2 - w_1)/\pi$, the $\{v_m^n(N, \beta_k)\}$ are the DPSS's designed for bandwidth β_k in normalized hertz ([0, .5] Hz) and length N, $\beta_k = T_k \Delta w / 2\pi$, and the α_n^k are scalars.

Our argument starts with the observation that since $h_k(t)$ can be expressed as

$$h_k(t) = \frac{1}{2\pi} \int H_k(w) e^{iwt}\, dw \quad , \qquad (5)$$

it can be regarded as a "Fourier transform" of the "waveform" $H_k(w)$ ($h_k(t)$ is the complex conjugate of the Fourier transform of $\frac{1}{2\pi} H_k(w)$). If $h_k(t)$ lies in some time interval $[-T_k, T_k]$, we can say that the "waveform" $H_k(w)$ is approximately bandlimited. By the relationship between time and frequency, it can be shown that the normalized bandwidth is $\beta_k = T_k \Delta w / 2\pi$. Also, it is well known that a sequence of N samples from a low pass stationary random process with a rectangular power spectrum of bandwidth β_k and sampled at rate f_s can be accurately approximated using a linear expansion of only $\frac{2\beta_k}{f_s} N$ DPSS's [7] (see also [6] about the approximate dimension of a bandlimited signal and its expansion using the DPSS's). Hence from the above discussion, we infer that the sequence $H_k(w_1 + m\Delta)$ should roughly be representable using a linear expansion of about r_k terms where

$$r_k = \frac{2T_k}{f_s} N \qquad (6)$$

and $f_s = 2\pi/\Delta w$. Formula (6) can be simplified by noting that as $\Delta w \to 0$, it tends to

$$r_k = 2T_k(w_2 - w_1) \qquad (7)$$

which should only be used as an heuristic rule or bound to gain rough insight into the dimensionality. r_k should be more precisely determined by experimentation.

We now substitute (4) into (3) to get

$$\min_{\{\tau_k\},\{\alpha_j^k\}} \sum_m |D(w_m) - \sum_{k=1}^{M} e^{-i\tau_k w_m} \sum_{j=1}^{r_k} \alpha_j^k v_m^j(N, \beta_k) S(w_m)|^2. \qquad (8)$$

The original constrained optimization problem is now an unconstrained optimization problem in terms of the α_j^k and τ_k because the unknown shape of the $h_k(t)$ is now represented in terms of the linear parameters α_j^k in (8). This greatly simplifies the optimization problem. It will be helpful to rewrite (8) in vector notation as

$$\min_{\tau_1,\ldots,\tau_M,\mathbf{a}_1,\ldots,\mathbf{a}_M} \|\mathbf{d} - \sum_{k=1}^{M} W(\tau_k) V_k \mathbf{a}_k\|_F^2 \qquad (9)$$

where

$$\mathbf{d} = [D(w_1)\ D(w_1 + \Delta w) \cdots D(w_1 + (N-1)\Delta w)]^T. \qquad (10)$$

$W(\tau_k)$ is a $N \times N$ diagonal matrix whose elements are $w_{m,m} = S(w_1 + (m-1)\Delta w) e^{-i\tau_k(w_1 + (m-1)\Delta w)}$, the V_k are $N \times r_k$ matrices whose columns are the DPSS's, and

$$\mathbf{a}_k = [\alpha_1^k\ \alpha_2^k \cdots \alpha_{r_k}^k]^T. \qquad (11)$$

Solving for the τ_k

To estimate the τ_k, we need to solve (9). Direct minimization of (9) is difficult. We propose to use an approach which was originally proposed in [4] and modified in [5] which decomposes the original signal into its constituent components and then estimates the parameters of the individual components separately through a sequence of one-dimensional searches. The approach accounts for the bias in the estimates by matching each search to its corresponding distorted residual signal [5]. We now present a brief derivation of the algorithm.

In each iteration, we solve

$$\min_{\tau_m,\{\mathbf{a}_m\}} \|\mathbf{d} - \sum_{k=1,k\neq m}^{M} W(\tau_k^h) V_k \mathbf{a}_k - W(\tau_m) V_k \mathbf{a}_m\|_F^2 \qquad (12)$$

where the τ_k^h are the estimates from the hth step. Note that the minimization is done with respect to only the

mth arrival time, τ_m, but with all the $\mathbf{a}_k$. Following [5], the linear parameters $\mathbf{a}_k$ can be eliminated to obtain the equivalent one dimensional minimization

$$\min_{\tau_m} \|(I - P(\tau_m))\mathbf{d}\|_F^2 \tag{13}$$

where $P(\tau_m)$ is a projection operator onto the column space of the $N \times M$ matrix

$$C = [B_1 \mid B_2 \mid \cdots \mid B_M] \tag{14}$$

where $B_k = W(\tau_k)V_k$. The projection operator $P(\tau_m)$ is given by

$$P(\tau_m) = C(C^H C)^{-1} C^H. \tag{15}$$

To simplify (13), we construct the $N \times M - 1$ matrix C_m by removing the mth column of C. It is easy to show that

$$Range(C) = Range(C_m) + Range(P_{C_m}^{\perp} B_m) \tag{16}$$

where $P_{C_m}^{\perp}$ is the projection operator onto the orthogonal complement of the column space of C_m. Then we can rewrite $P(\tau_m)$ as

$$P(\tau_m) = P_{C_m} + P_{A_m} \tag{17}$$

where

$$P_{C_m} = C_m({C_m}^H C_m)^{-1} {C_m}^H \tag{18}$$

and

$$P_{A_m} = A_m(A_m^H A_m)^{-1} A_m^H \tag{19}$$

with $A_m = P_{C_m}^{\perp} B_m$. Substituting (17) into (13) and explicitly evaluating the norm, the minimization of (13) can be rewritten as the maximization of

$$\max_{\tau_m} \mathbf{d}^H P_{A_m} \mathbf{d}. \tag{20}$$

A summary of the iterative procedure is as follows:

1) The iteration is initialized by assuming $M = 1$ and solving (20) for the first estimate $\tilde{\tau}_1$.
2) Next, we let $M = 2$ and $\tau_1 = \tilde{\tau}_1$ in (20) and solve for τ_2, holding τ_1 fixed. This step is repeated for $M = 3, 4 \ldots, K$ where K is the total number of paths. Note that in each step the previous estimates $\{\tilde{\tau}_k\}_{k=1,\ldots,M-1}$ are used in the evaluation of (20) and are kept fixed.
3) Once K initial estimates are obtained, we solve and update the estimates for τ_k one at time until the change in (20) is less than some desired convergence criterion.

This algorithm is an extension of the Fast Maximum Likelihood (FML) procedure [4, 8] to incorporate orthogonal bases. We reduce the computational requirements of FML by using orthogonal components so that the estimation of the parameters becomes decoupled. This approach is taken in [9] for estimating the frequencies of complex sinusoids. A detailed comparison between FML and the class of algorithms that iteratively maximize the likelihood function by updating the parameters of individual components is found in [4].

III. EXPERIMENTAL RESULTS

We consider a two path example in which the received data is modeled as

$$d_n = \underbrace{h_n * s_n}_{\text{spread channel}} + 2s_{n-59} + w_n \tag{21}$$

for $n = 0, 1, \ldots, 1023$ where w_n is a IID zero-mean complex Gaussian distributed noise sequence. The spread channel h_n is plotted in figure 1 and is modeled as a cluster of very closely spaced discrete paths (spacing is half the sampling rate). For example, h_n can arise from an extended reverberator.

The transmitted signal is a linear sweep FM given by

$$s_n = e^{i2\pi \frac{93}{199} n^2} \tag{22}$$

for $n = 0, 1, \ldots, 199$. The main-lobe width of the signal autocorrelation function is approximately 36 samples. Note that the sampling rate is one second.

A single realization of data was computer generated according to formula (21) with noise variance 48.8. The data was transformed to the frequency domain by a 1024 point FFT and bins 1-60 were used. The reconstructed raw data from bins 1-60 is plotted in figure 2. The spread channel was represented using the first two DPSS's designed for bandwidth 20/1024.

For this particular example the algorithm converged in 3 iterations. The estimates we obtained were $\tau_1 = .4$ (spread channel) and $\tau_2 = 54.4$ (discrete path). The residual after the estimated components are removed from the data is plotted in figure 2. Note that the estimates are quite close and that the discrete path is not resolved by the matched filter (see figure 2). For comparison, we repeated the example assuming that only discrete paths are present. After 4 iterations we obtained $\tau_1 = 4.48$ and $\tau_2 = 14.08$. Note that the discrete path at delay 59 is not resolved.

IV. SUMMARY

Motivated by the difficulty of matched filtering and standard high resolution algorithms to accurately estimate the arrival times of signals that have propagated via temporally spread channels, we have proposed a frequency–domain estimation procedure based

on maximum likelihood that features a DPSS expansion to model the unknown channel spreading. The iterative estimation algorithm decomposes the original data into orthogonal individual components, provides a specific procedure for initialization, and improves on the estimates of the parameters in a well-defined and sequential manner. The computational efficiency of the algorithm is derived from the use of orthogonal basis vectors combined with the use of only one-dimensional searches in the parameter domain. For future work, an investigation of the proposed algorithm's convergence properties is required.

The combined spread and discrete channel example that we present demonstrates that it is important to take channel spreading into account and shows that the proposed modeling procedure can lead to significantly improved arrival time estimation.

REFERENCES

[1] I.P. Kirsteins, "High resolution time delay estimation," in *Proc. IEEE International Conference on Acoustics, Speech, and Signal Proc.*, pp. 451-454, 1987.

[2] I.P. Kirsteins and A.H. Quazi, "Exact Maximum Likelihood Time Delay Estimation for Deterministic Signals," in *Proc. of Eusipco-88*, Grenoble, France, Sept. 1988.

[3] R.J. Vaccaro, C.S. Ramalingam, and D.W. Tufts, "Least-squares time-delay estimation for transient signals in a multipath environment," *J. Acoust. Soc. Am.*, vol. 92(1), pp. 210-218, July 1992.

[4] S. Umesh, "Fast maximum likelihood estimation of parameters in crowded signal environments," Ph.D. dissertation, Univ. of Rhode Island, Kingston, RI, Aug. 1993.

[5] G.S. Edelson and D.W. Tufts, "Approximately unbiased maximum likelihood estimation of reverberation components," presented at the *1993 IEEE Underwater Acoustics Signal Processing Workshop*, West Greenwich, RI, Oct. 1993.

[6] D. Slepian, "Prolate spheroidal wave functions, Fourier analysis, and uncertainty - V: the discrete case," BSTJ, vol. 57, no. 5, pp. 1371-1430, May-June 1978.

[7] L.L. Scharf, "The SVD and reduced rank signal processing," *Signal Processing*, vol. 25, pp. 113-133, 1991.

[8] D.W. Tufts, H. Ge, and S. Umesh, "Fast maximum likelihood estimation of signal parameters using the shape of the compressed likelihood function," *IEEE J. Oceanic Eng.*, vol. 18, pp. 388-400, Oct. 1993.

[9] J-K Hwang and Y-C Chen, "Superresolution frequency estimation by alternating notch periodogram," *IEEE Trans. Sig. Proc.*, vol. 41, pp. 727-741, Feb. 1993.

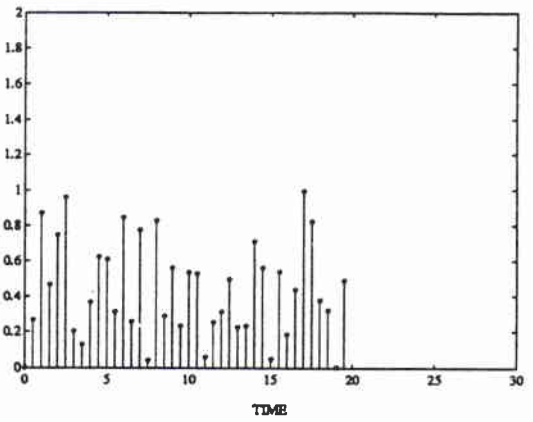

Figure 1. Spread channel impulse response.

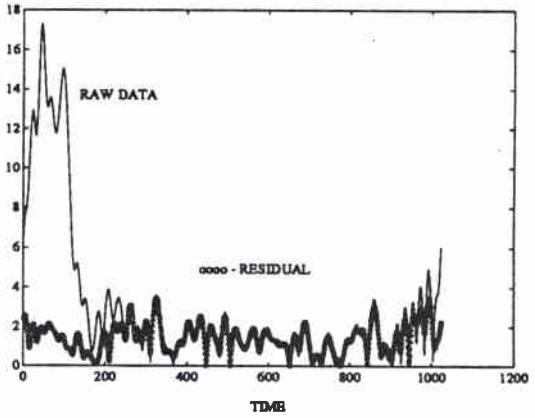

Figure 2. Envelope of raw data and residual.

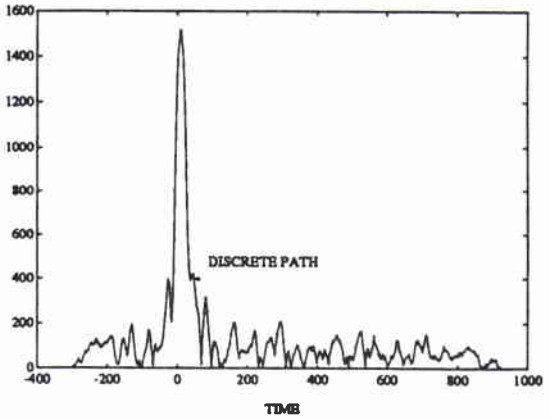

Figure 3. Envelope of matched filter output.

Annex III

Analysis and interpretation of the reduced-rank generalized likelihood-ratio test

The paper reproduced in this annex was originally published as:

Kirsteins, I. (1994) Analysis and interpretation of the reduced-rank generalized likelihood-ratio test. *In*: Holt, M.J.J., Cowan, C.F.N., Grant, P.M., Sanham, W.A., *eds*., Signal Processing VII Theories and Applications. Proceedings of EUSIPCO-94, seventh European Signal Processing Conference, Edinburgh, 13–16 September, 1994, Vol. I. Lausanne, European Association for Signal Processing, 1994.

intentionally blank page

SIGNAL PROCESSING VII: Theories and Applications
M. Holt, C. Cowan, P. Grant, W. Sandham (Eds.)
© 1994 European Association for Signal Processing

Report no. changed (Mar 2006): SM-287-UU

Analysis and Interpretation of the Reduced-Rank Generalized Likelihood-Ratio Test

Ivars P. KIRSTEINS

SACLANT Undersea Research Centre, Viale San Bartolomeo 400, 1-19138 La Spezia, Italy

Abstract. An analysis and interpretation of the reduced-rank generalized likelihood-ratio test (RR-GLRT) detector is presented in this paper. First, simple and accurate approximations to the RR-GLRT test statistics are derived. The approximations are verified by computer simulation and are shown to be accurate over a wide range of interference and signal levels. These approximations are then used to show that the RR-GLRT is related to the UMP invariant test and to calculate the moments and deflection of the RR-GLRT statistic.

1. Introduction

The objective here is to analyse and provide an interpretation of the recently proposed reduced-rank generalized likelihood-ratio test (RR-GLRT) [1, 2] for detecting a low rank signal in the presence of unknown, strong low rank interference plus white Gaussian noise. The RR-GLRT leads to a test which is similar in spirit to the Principal Component Inverse (PCI) method [3] of rapidly adaptive detection and extends the PCI method to the case where the training data is contaminated by signal components. Computer simulations indicate that the RR-GLRT performs well [1, 2]. We begin with a review of the detection scenario.

Let us assume that K independent, complex-valued, $m \times 1$ data vectors or "snapshots" of data $\{\mathbf{x}_1, \ldots, \mathbf{x}_K\}$ are observed consisting of either interference or interference plus signal. In [2] the RR-GLRT was derived for two different distribution models. In both cases, the snapshots are modeled as complex multivariate Gaussian distributed, but with different assumptions. In the first case, the low rank interference component is modeled as deterministic. Here, the distributions for the interference only and interference plus signal hypotheses are:

$$\mathcal{H}_0: \quad \mathbf{x}_k \sim N_C(H\mathbf{b}_k, \sigma^2 I) \quad , \quad k = 1, \ldots, K \qquad (1)$$

$$\mathcal{H}_1: \quad \mathbf{x}_k \sim N_C(H\mathbf{b}_k + S\mathbf{c}_k, \sigma^2 I) \quad , \quad k = 1, \ldots, K \qquad (2)$$

where the columns of the $m \times r_h$ matrix H and $m \times r_s$ matrix S generate the low rank interference and signal spaces respectively, and the elements of the vectors $\mathbf{b}_k$ and $\mathbf{c}_k$ are the scale factors for the kth realization of interference and signal respectively. We assume that H, $\mathbf{b}_k$, $\mathbf{c}_k$, and σ^2 are unknown.

In the second case, the low rank interference component is modeled as complex multivariate Gaussian distributed. Here, the distributions for the interference only and interference plus signal hypotheses are:

$$\mathcal{H}_0: \quad \mathbf{x}_k \sim N_C(\mathbf{0}, Q + \sigma^2 I) \quad , \quad k = 1, \ldots, K \qquad (3)$$

$$\mathcal{H}_1: \quad \mathbf{x}_k \sim N_C(S\mathbf{c}_k, Q + \sigma^2 I) \quad , \quad k = 1, \ldots, K \qquad (4)$$

where Q is the rank r_h covariance matrix of the low rank interference component. We assume that Q, σ^2 and $\mathbf{c}_k$ are unknown.

We now review the RR-GLRT detectors. For further detail the reader is referred to [1, 2]. The GLRT is derived by constructing the LRT for choosing between hypotheses $\mathcal{H}_0$ and $\mathcal{H}_1$ and then replacing the unknown parameters by their ML estimates. We begin with the deterministic case.

Deterministic Low Rank Interference

For convenience, $\{\mathbf{x}_k\}$, $\{\mathbf{c}_k\}$, and $\{\mathbf{b}_k\}$ are arranged column-wise into the matrices X, C and B respectively. Note that in matrix form, the low rank interference and signal components are HB and SC. Thus the unknown parameters in the joint PDF of X are H, B, C, and the white noise variance σ^2. It can be shown that a GLRT statistic for this case is [1, 2]

$$z_1 = \frac{\max_{H,B,C,\sigma^2} \frac{1}{\sigma^{mK}} exp\left(-\frac{1}{\sigma^2}\|X - HB - SC\|_F^2\right)}{\max_{H,B,\sigma^2} \frac{1}{\sigma^{mK}} exp\left(-\frac{1}{\sigma^2}\|X - HB\|_F^2\right)} \qquad (5)$$

The test statistic (5) simplifies to [1, 2]

$$z_1 \propto \frac{\|X - \hat{X}_{r_h}\|_F^2}{\|P_S^{\perp} X - \hat{X}_{S r_h}\|_F^2} \tag{6}$$

where $\hat{X}_{r_h}$ and $\hat{X}_{S r_h}$ are the best rank r_h approximations to X and $P_S^{\perp} X$ in the least-squares sense respectively. $P_S^{\perp}$ is the projection operator onto the orthogonal complement of the column space of S.

Gaussian Low Rank Interference

The unknown parameters in the PDF are now the covariance matrix Q of the low rank interference component, C , and the white noise variance σ^2. Note that we must constrain the rank of Q to r_h when estimating the parameters.

Following the same steps as before, it can be shown that a GLRT test statistic is [2]

$$z_2 = \frac{\max_{Q,\sigma^2,C} |Q_1+\sigma^2|^{-K} \exp\left(-K\, trace(Q+\sigma^2 I)^{-1}\hat{R}_1\right)}{\max_{Q,\sigma^2} |Q+\sigma^2|^{-K} \exp\left(-K\, trace(Q+\sigma^2 I)^{-1}\hat{R}_0\right)} \tag{7}$$

where $\hat{R}_0 = \frac{1}{K} X X^H$ and $\hat{R}_1 = \frac{1}{K}(X - SC)(X - SC)^H$.

Formula (7) simplifies to [2]

$$z_2 \propto \left(\frac{\tilde{\lambda}_1^{H0} \tilde{\lambda}_2^{H0} \ldots \tilde{\lambda}_{r_h}^{H0}}{\tilde{\lambda}_1^{H1} \tilde{\lambda}_2^{H1} \ldots \tilde{\lambda}_{r_h}^{H1}} \right)^{1/(m-r_h)} z_1 \tag{8}$$

where the $\{\tilde{\lambda}_k^{H0}\}$ and $\{\tilde{\lambda}_k^{H1}\}$ are the eigenvalues of $\hat{R}_0$ and $P_S^{\perp} \hat{R}_0 P_S^{\perp}$ respectively.

In order to analyse the performance of the RR-GLRT, we require the statistics (eg., moments, density) of the test under $\mathcal{H}_0$ and $\mathcal{H}_1$. The statistics are difficult to obtain analytically because the test statistics are a function of the eigenvalues or singular values of the data matrix which are highly non-linear functions of data. In the next section we develop approximations to the test statistics which can be readily analysed.

2. Test Statistic Approximation

The approach we take is to use perturbation expansions for the low rank fitting error [3] and estimated signal subspace [4] to derive simple approximations to z_1 (6) and z_2 (8). The key assumption used is that the low rank interference component HB is much stronger than the signal component SC (when present) and the background noise N in the observed data $X = HB + SC + N$. That is, in the analysis, both SC and N are treated as perturbations. It is also pointed out that the analysis is done for a specific realization of interference HB and signal SC.

We now present an outline of the main steps involved in deriving the approximations to z_1 and z_2. For a discussion of the specific details involved in each step, the reader is referred to appendix A.

1) The perturbation expansion for the error in approximating a matrix by a matrix of lower rank derived in [3] is used to obtain the approximation

$$z_1 \approx 1 + \frac{\|P_{P_H^{\perp} S} X P_B^{\perp}\|_F^2}{\|P_{HS}^{\perp} X P_B^{\perp}\|_F^2} \tag{9}$$

where $P_{P_H^{\perp} S}$, $P_{HS}^{\perp}$, and $P_B^{\perp}$ are projection operators onto the column space of $P_H^{\perp} S$, orthogonal complement of the column space of $[H|S]$, and the orthogonal complement of the row space of the complex conjugate of B respectively.

2) Formula (8) can be rewritten as

$$z_2 \propto \left(\frac{|\tilde{U}_0^H \hat{R}_0 \tilde{U}_0|}{|\tilde{U}_1^H P_S^{\perp} \hat{R}_0 P_S^{\perp} \tilde{U}_1|} \right)^{1/(m-r_h)} z_1 \tag{10}$$

where the columns of $\tilde{U}_0$ and $\tilde{U}_1$ are the r principal eigenvectors of $\hat{R}_0$ and $P_S^{\perp} \hat{R}_0 P_S^{\perp}$, respectively.

3) The perturbation expansion derived in [4] for the estimated interference subspace is used to approximate the ratio of determinants in (10) as

$$\gamma = \frac{|\tilde{U}_0^H \hat{R}_0 \tilde{U}_0|}{|\tilde{U}_1^H P_S^{\perp} \hat{R}_0 P_S^{\perp} \tilde{U}_1|} \approx \frac{|U_0^H \hat{R}_0 U_0|}{|U_1^H \hat{R}_0 U_1|} \tag{11}$$

where the orthonormal columns of U_0, U_1 span the column spaces of H and $P_S^{\perp} H$ respectively.

4) The ratio of determinants (11) is now approximated using a first-order Taylor expansion as

$$\gamma \approx \frac{|Q_0|}{|Q_1|} \left(1 + \frac{\Delta}{K}\right) \tag{12}$$

where
$\Delta = trace[Q_0^{-1} U_0^H X X^H U_0] - trace[Q_1^{-1} U_1^H X X^H U_1]$,
$Q_0 = U_0^H E E^H U_0 / K + \sigma^2 I$,
$Q_1 = U_1^H E E^H U_1 / K + \sigma^2 I$, and $E = HB$.

5) When N is small, the term Δ/K also becomes small. Then, for small N, $(1+\frac{\Delta}{K})^{(1/(m-r_h)} \approx 1 + \Delta/K(m-r_h)$. Substituting the above approximation and (9) into (10), we obtain the approximation

$$z_2 \approx \frac{|Q_0|}{|Q_1|}^{1/(m-r_h)} \left(1 + \frac{\Delta}{K(m-r_h)} + \frac{\|P_{P_H^{\perp} S} X P_B^{\perp}\|_F^2}{\|P_{HS}^{\perp} X P_B^{\perp}\|_F^2} + \frac{\Delta}{K(m-r_h)} \frac{\|P_{P_H^{\perp} S} X P_B^{\perp}\|_F^2}{\|P_{HS}^{\perp} X P_B^{\perp}\|_F^2}\right) \tag{13}$$

Summarizing, we have derived accurate approximations for z_1 and z_2 which are given by formulas (9) and

(13) respectively. In the next section we discuss the relationship of the RR-GLRT to optimum detectors.

3. Interpretation of the RR-GLRT and Calculation of the Mean and Variance

The above approximations provide useful insight about the RR-GLRT detectors. Note that in the following discussions we assume that the elements of N are IID complex Gaussian distributed with zero-mean and variance σ^2. We began with the connection of z_1 (9) to the UMP invariant test for detecting a subspace signal in subspace interference and white noise of unknown variance. Scharf [5] showed that (here modified for the multiple snapshot case)

$$1 + \frac{\|P_{P_H^\perp S} X\|_F^2}{\|P_{HS}^\perp X\|_F^2} \underset{\mathcal{H}0}{\overset{\mathcal{H}1}{\gtrless}} \eta \qquad (14)$$

(η is some threshold) is the UMP test invariant to rotations in the range of $P_{P_H^\perp S}$ and non-negative scalings of X. Note that (14) and (9) are almost identical except for the post-multiplication of X by $P_B^\perp$. The post-multiplication of X by $P_B^\perp$ can be interpreted as a loss due to the low rank estimation procedure. However, when r_h is small, we expect the loss to be generally small since the projection operator $P_B^\perp$ is almost of full rank.

For insight into z_2 (13) we replace $\|P_{HS}^\perp X P_B^\perp\|_F^2$ by its expected value $\sigma^2(m - r_h - r_s)(K - r_h)$ and assume that m and K are large. Then (13) becomes approximately

$$z_2 \equiv trace[Q_0^{-1} U_0^H X X^H U_0] + \frac{\|P_{P_H^\perp S} X P_B^\perp\|_F^2}{\sigma^2} - trace[Q_1^{-1} U_1^H X X^H U_1] + \Delta \frac{\|P_{P_H^\perp S} X P_B^\perp\|_F^2}{\sigma^2} \qquad (15)$$

where scale factors and constants have been removed. We now compare (15) to the Gauss-Gauss detector for the case when the dimensionality of the observed data has been reduced by projection onto the column space of $[H|S]$, e.g., $Z = [U_0|U_S]^H X$ where the orthonormal columns of U_S generate the column space of $P_H^\perp S$. Assuming the signal is strong and of dimension $r_h + r_s$ (we are assuming an arbitrary signal here, not the signal defined previously), a test statistic for Z is (see [7])

$$z = trace[Q_0^{-1} U_0^H X X^H U_0] + \frac{\|P_{P_H^\perp S} X\|_F^2}{\sigma^2} \qquad (16)$$

where Q_0 is the covariance matrix of $U_0^H \mathbf{x}_k$. Note that the first two terms of (15) are very similar to (16). It is not directly obvious how the last two terms in (15) affect performance. This has to be studied further. Finally, we note that $\Delta = 0$ and hence $z_2 \approx z_1$ when the signal is orthogonal to the interference, i.e., $S^H H = 0$.

It is now pointed out that z_2 utilizes signal components which lie in the range of H, while z_1 does not. Thus, we conjecture that the test based on z_2 should perform better.

Calculating the mean and variance of z_1 (9) is straight forward. It is easy to show that $z_1 - 1$ is distributed as $(v_1/v_2)F_{v_1,v_2}$ under hypothesis $\mathcal{H}0$ and $(v_1/v_2)F(\beta)_{v_1,v_2}$ under $\mathcal{H}1$ where $v_1 = 2r_s(K - r_h)$, $v_2 = 2(m - r_h - r_s)(K - r_h)$, and $\beta = 2\|P_{P_H^\perp S} S P_B^\perp\|_F^2/\sigma^2$ (see [6] for discussion on F distributions). The mean and variance can then be obtained from the tables in [6].

The calculation of the mean and variance of z_2 is more difficult because the term $Q_1^{-1} U_1^H X X^H U_1$ and the numerator of $z_1 - 1$ (9) are correlated to some degree. However, in practice we have found the correlation to be very small and that $\gamma^{1/(m-r_h)}$ and z_1 can be approximated as uncorrelated. Thus, the mean and variance of z_2 can be obtained by first calculating the mean and variance of $\gamma^{1/(m-r_h)}$ using some results found in [8] and then assuming that z_1 and $\gamma^{1/(m-r_h)}$ in the product $z_1 \gamma^{1/(m-r_h)}$ are uncorrelated.

4. Experimental Results

In the simulations, a twenty sensor equi-spaced line array is used to detect a plane wave monochromatic signal arriving at broadside. The interference consists of two strong, far-field equi-powered monochromatic jammers located in bearing symetrically about broadside plus a background white Gaussian noise component.

20 independent snapshots of the low rank interference component and 20 signal snapshots were generated where $\|HB\|_F^2 = 42.2$ and $\|SC\|_F^2 = 1.4$. In each trial, the true and approximate test statistics are evaluated using the same realization of low rank interference and signal, but with independent realizations of the background white Gaussian noise with variance .01.

A total of 200 independent trials were performed with the low rank interference spatial frequency (separation from signal component) varied from 1 to .5 DFT bin-widths. In figure 1 the theoretically calculated means and variances for hypothesis $\mathcal{H}1$ are compared against the experimentally measured values. They agree quite well. Although not presented here, the true and approximate test statistics were also compared by scattergrams. Here also, the true and approximate test statistics were very close.

The above approximations can now be used to evaluate the deflection

$$d = \frac{(E^{\mathcal{H}1}[z] - E^{\mathcal{H}0}[z])^2}{.5(\mathrm{Var}^{\mathcal{H}0}[z] + \mathrm{Var}^{\mathcal{H}1}[z])} \qquad (17)$$

which is an indicator of receiver performance. The deflections are plotted in figure 2 and compared against the UMP invariant receiver (14). Note that the deflection of z_1 is close to the UMP invariant test and that z_2 is somewhat higher than z_1.

5. Conclusion

Accurate approximations have been derived for the RR-GLRT receivers which provide useful insight about the receiver structures and are simple to analyse statistically. In future work the analysis will be considered for the case of random low rank interference and signal components, rather than for fixed realizations of HB and SC.

Appendix A

Step 1: Using the perturbation expansion derived in [3] for the error in approximating a matrix by a matrix of lower rank and keeping only first-order terms, it can be shown that

$$\|X - \hat{X}_r\|_F^2 \approx \|P_H^{\perp} X P_B^{\perp}\|_F^2 \qquad (18)$$

and

$$\|P_S^{\perp} X - \hat{X}_{r\perp}\|_F^2 \approx \|P_{P_S^{\perp} H}^{\perp} P_S^{\perp} X P_B^{\perp}\|_F^2 \qquad (19)$$

where $P_H^{\perp}$ is the projection operator operator onto the orthogonal complement of the column space of H.

Next, using the relationship $P_S + P_{P_S^{\perp} H} + P_{HS}^{\perp} = I$ (where P_S is the projection operator onto the column space of S), (19) can be rewritten as

$$\|P_S^{\perp} X - \hat{X}_{r\perp}\|_F^2 \approx \|P_{HS}^{\perp} X P_B^{\perp}\|_F^2 \qquad (20)$$

Similarily, noting that $P_H + P_{P_H^{\perp} S} + P_{HS}^{\perp} = I$, (18) can be rewritten as

$$\|X - \hat{X}_r\|_F^2 \approx \|P_{P_H^{\perp} S} X P_B^{\perp}\|_F^2 + \|P_{HS}^{\perp} X P_B^{\perp}\|_F^2 \qquad (21)$$

Substituting (21) and (20) into (6), we obtain the approximation (9).

Step 3: A first-order perturbation expansion of the space spanned by the r principal left singular vectors of a perturbed matrix $\tilde{R} = R + \Delta R$, where $rank[R] = r$, is [4]

$$\tilde{U}_I \approx U_I + (I - U_I U_I^H) \Delta R U_I \Lambda_I^{-1} \qquad (22)$$

where the columns of U_I are the r principal left singular vectors of R and Λ_I is a diagonal matrix of the principal singular values. Substituting (22) into $\tilde{U}_I^H (R + \Delta R) \tilde{U}_I$ and keeping only first-order terms, we get $\tilde{U}_I^H (R + \Delta R) \tilde{U}_I \approx U_I^H \tilde{R} U_I$. This approximation is then used to obtain (11).

Step 4: The first-order Taylor expansion of the ratio of two determinants $|Q_0 + \Delta Q_0| / |Q_1 + \Delta Q_1|$, about matrices Q_0 and Q_1,

$$\frac{|Q_0 + \Delta Q_0|}{|Q_1 + \Delta Q_1|} \approx \frac{|Q_0|}{|Q_1|} \left(1 + trace[\Delta Q_0^T (Q_0^{-1})^T] - trace[\Delta Q_1^T (Q_1^{-1})^T] \right) , \qquad (23)$$

is obtained by direct application of the standard formula for the partial derivative of a determinant [9]. Letting $\Delta Q_0 = U_0^H X X^H U_0 / K - Q_0$ and $\Delta Q_1 = U_1^H X X^H U_1 / K - Q_1$ in (23) and after some manipulation, we get (12).

References

[1] I.P. Kirsteins, "A Reduced-Rank Generalised Likelihood-Ratio Test," in Proc. of the 1992 NATO ASI Conference on Underwater Acoustic Signal Processing, Madiera Island, Portugal.

[2] I.P. Kirsteins, "A reduced-rank generalised likelihood ratio test," technical memorandum, NUWC Detachment, New London, CT, USA, March 1992.

[3] I.P. Kirsteins and D.W. Tufts, "Adaptive detection using low rank approximation to a data matrix," IEEE Trans. Aerospace and Elect. Sys., Vol. 30, No. 1, pp. 55-67, Jan. 1994.

[4] D.W. Tufts, "The effects of perturbations on matrix-based signal processing," in Proc. of Fifth ASSP workshop on Spectr. Est. and Mod., pp. 159-162, 1990.

[5] L.L. Scharf and B. Friedlander, "Matched subspace detectors," submitted to IEEE Trans. in Sig. Proc., June 1993.

[6] N.L. Norman and S. Kotz, Continous univariate distributions-2, John Wiley and Sons, New York, 1970.

[7] R.N. McDonough, "A canonical form of the likelihood detector for Gaussian random vectors," JASA, Vol. 49, No. 2 (part 1), pp.402-406, 1971.

[8] J.A. Tague and C.I. Caldwell, "Expectations of useful complex wishart forms," Ohio University technical report, Athens, OH. 1993.

[9] R.J. Tallarida, Pocket Book of Integrals and Mathematical Formulas, 2nd Edition, CRC Press, Ann Arbor, 1992.

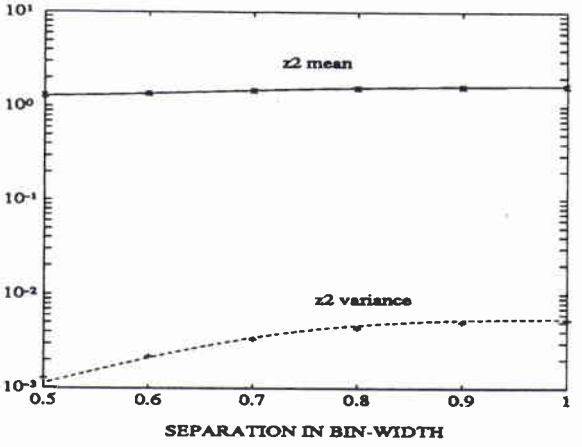

Figure 1. Calculated and experimentally measured (x - mean, + - variance) mean and variance.

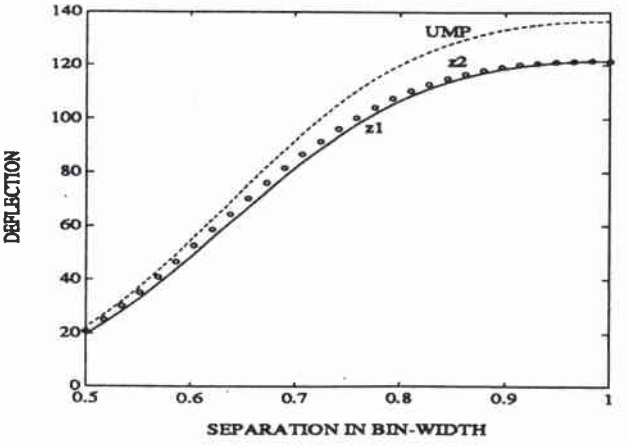

Figure 2. Calculated deflection

Document Data Sheet

Security Classification		Project No.
NATO UNCLASSIFIED		02
Document Serial No.	**Date of Issue**	**Total Pages**
SM-287	April 1995	18 pp.

Author(s)

I.P. Kirsteins

Title

Reverberation suppression

Abstract

We propose a processing methodology for shallow-water reverberation suppression in which acoustic propagation and scattering physics are used as a *guide* to develop simple, but still accurate representations for the received data which are motivated by the ease of development of efficient signal-processing algorithms. The methodology is demonstrated by showing that temporally spread reverberation components can be accurately modeled using a reduced-rank representation and expansion by discrete prolate spheroidal sequences. These representations lead to the application of the Principal Component Inverse (PCI) method and the reduced-rank generalized likelihood-ratio test (RR-GLRT) for suppressing reveberation and the development of an iterative scheme for estimating arrival times in the presence of temporally spread reverberation components. We also present a performance analysis of the RR-GLRT. Using both simulated and real data, it is shown that these methods perform well.

Keywords

adaptive detection, generalized likelihood-ratio test, performance assessment, reduced-rank interference cancellation, reverberation suppression, time delay estimation

Issuing Organization

North Atlantic Treaty Organization
SACLANT Undersea Research Centre
Viale San Bartolomeo 400, 19138 La Spezia, Italy

[From N. America: SACLANTCEN CMR-426 (New York) APO AE 09613]

tel: +39-187-540.111
fax: +39-187-524.600

e-mail: sti@saclantc.nato.int

Initial Distribution for SM-287

SCNR for SACLANTCEN	
SCNR Belgium	1
SCNR Canada	1
SCNR Denmark	1
SCNR Germany	1
SCNR Greece	1
SCNR Italy	1
SCNR Netherlands	1
SCNR Norway	1
SCNR Portugal	1
SCNR Spain	1
SCNR Turkey	1
SCNR UK	1
SCNR US	2
French Delegate	1
SECGEN Rep. SCNR	1
NAMILCOM Rep. SCNR	1

National Liaison Officers	
NLO Belgium	1
NLO Canada	1
NLO Denmark	1
NLO Germany	1
NLO Italy	1
NLO Netherlands	1
NLO UK	3
NLO US	4

Total external distribution	30
SACLANTCEN Library	20
Total number of copies	50